Bioorganic & Medicinal Chemistry Letters 20 (2010) 6865–6881

Contents lists available at ScienceDirect

Bioorganic & Medicinal Chemistry Letters

journal homepage: www.elsevier.com/locate/bmcl

Bioorganic & Medicinal Chemistry Letters Volume 20, Issue 23, 2010

Contents

ARTICLES

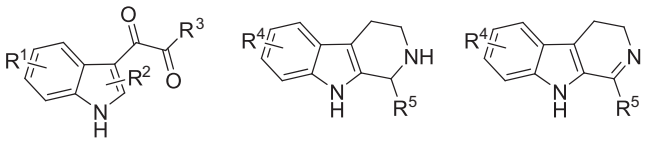

Synthetic analogs of natural products with enhanced activities against SrtA and ICL.

The synthesis and structure–activity relationships (SAR) of p38α MAP kinase inhibitors based on a 5-amino-pyrazole scaffold are described. These studies led to the identification of compound **2j** as a potent and selective inhibitor of p38α MAP kinase with excellent cellular potency toward the inhibition of TNFα production. Compound **2j** was highly efficacious in vivo in inhibiting TNFα production in an acute murine model of TNF production. X-ray co-crystallography of a 5-amino-pyrazole analog **2f** bound to unphosphorylated p38α is also disclosed.

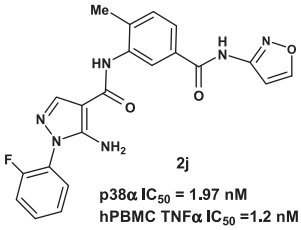

By using a small atom (Cl, F, or Me) to increase the torsion angle between the phenyl ring and the attached secondary amide, trifluoromethylphenyl motif was applied successfully as P2 for aldehyde/ketoamide-based cathepsin S inhibitors.

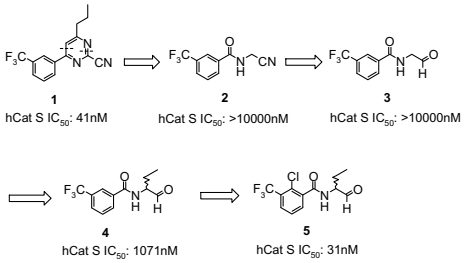

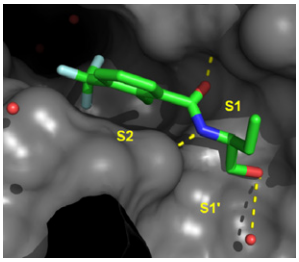

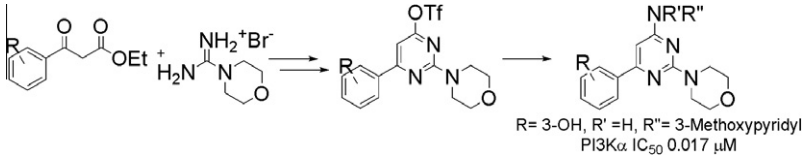

2-Morpholino pyrimidines inhibitors of PI3 kinase.

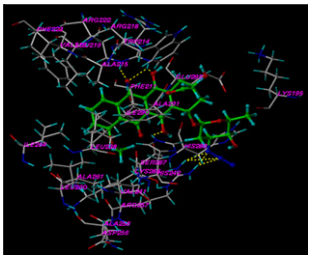

Site I is large enough to accommodate ADNR molecule and residues of HSA, ALA215, and HIS288 are in close proximity to ADNR suggesting the existence of hydrophobic interaction between them.

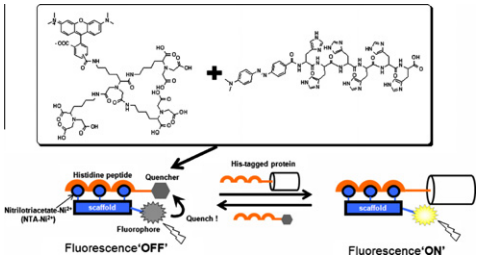

A new type of a 'turn-on' fluorescent probe for His-tagged proteins was constructed using tetramethylrhodamine-conjugated nitrilotriacetate derivative and Dabcyl-conjugated hexahistidine peptide.

Series of spiro-thiadiazoline derivatives of piperidines were synthesized and characterised. All the compounds were evaluated for in vitro antibacterial potency by serial dilution method, which is explained through QSAR studies.

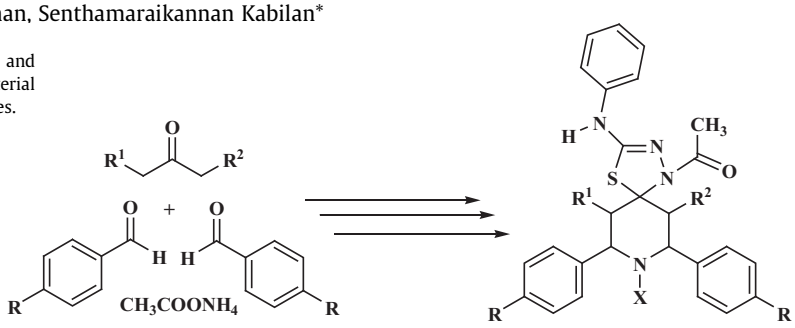

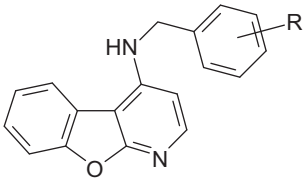

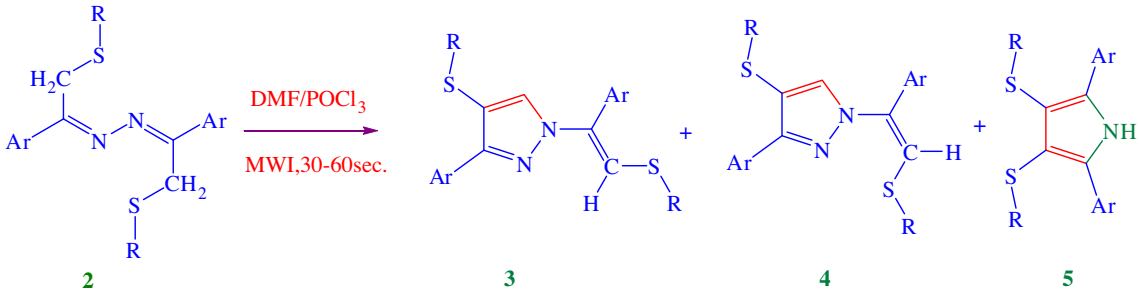

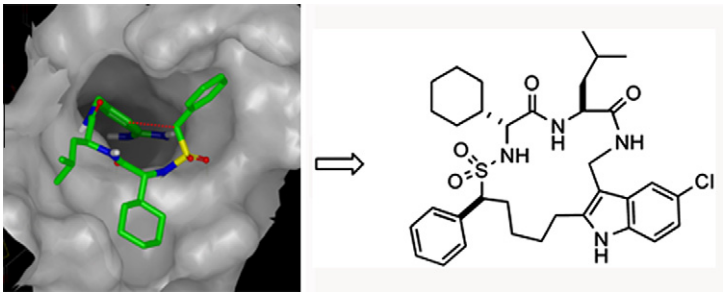

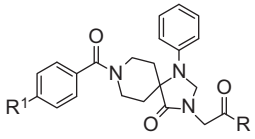

Ezetimibe (Zetia®), a cholesterol-absorption inhibitor (CAI) approved by the FDA for the treatment of hypercholesterolemia, is believed to target the intestine protein Niemann-Pick C1-Like 1 (NPC1L1) or its pathway. A spiroimidazolidinone NPC1L1 inhibitor identified by virtual screening showed moderate binding activity but was not efficacious in an in vivo rodent model of cholesterol absorption. Synthesis of analogs established the structure–activity relationships for binding activity, and resulted in compounds with in vivo efficacy, thereby providing proof-of-concept that non-β-lactams can be effective CAIs.

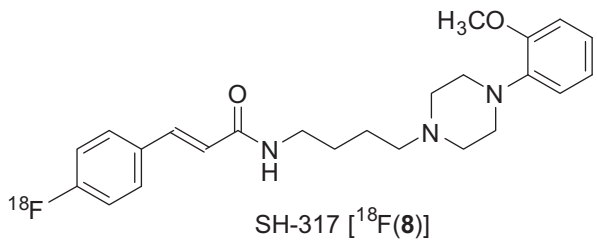

SH-317 [^{18}F(**8**)]

Radical ^{18}F-fluoroarylation with fluorine-18-labelled arenediazonium chlorides has been successfully applied to the radiochemical synthesis of the dopamine D_3-selective ligand SH 317 ([^{18}F]**8**). SH 317 has been evaluated as a new PET ligand candidate by in vivo experiments.

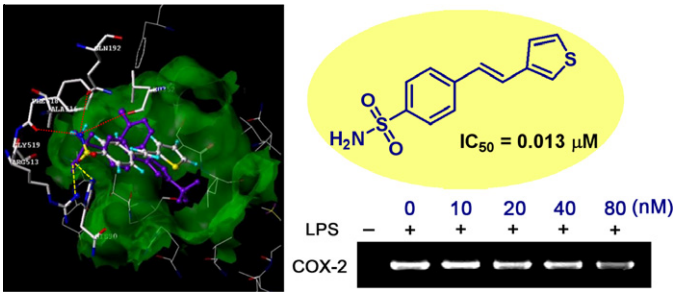

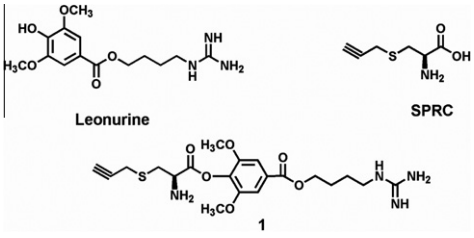

The synthesis and biological evaluation of novel leonurine–SPRC conjugate, 3,5-dimethoxy-4-(2-amino-3-prop-2-ynylsulfanyl-propionyl)-benzoic acid 4-guanidino-butyl ester (**1**) is reported in this Letter. It is designed to improve the pharmacology efficiency by combining leonurine with *S*-propargyl cysteine (SPRC), a cysteine analog, via a phenolic hydroxyl ester bond, which could be readily hydrolyzed to release bioactive leonurine and SPRC. Pharmacological evaluation has shown that **1** possesses potent cardioprotective effect against hypoxia-induced neonatal rat ventricular myocytes damage at lower molar concentration (10-fold less than leonurine required and 100-fold less than SPRC required). The mechanism is in partial related to improve hydrogen sulfide production, anti-oxidative stress and anti-apoptosis.

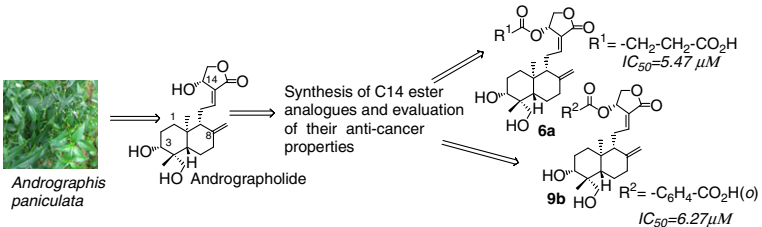

A series of analogues of andrographolide, prepared through chemo-selective functionalization at C14 hydroxy, have been evaluated for in vitro cytotoxicities against human leukemic cell lines. Two of the analogues (**6a**, **9b**) exhibited significant potency. Preliminary studies on structure–activity relationship (SAR) revealed that the α-alkylidene-γ-butyrolactone moiety of andrographolide played a major role in the activity profile. The structures of the analogues were established through spectroscopic and analytical data.

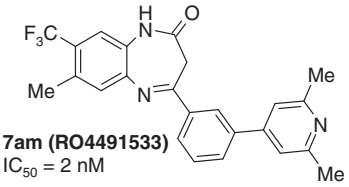

A series of 1,3-dihydro-benzo[*b*][1,4]diazepin-2-ones was finally developed into highly drug-like non-competitive group II mGluR antagonists. After oral administration of, for example, **7am** in vivo activity by reversal of the LY354740-induced hypolocomotion in rats and improvement of memory deficit in the DMTP task—also synergistically with donepezil—could be demonstrated.

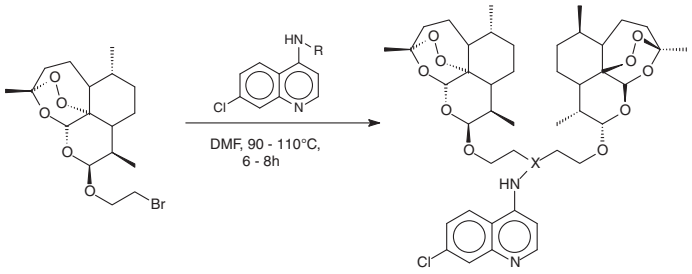

Novel artemisinin–quinoline dimers were synthesized upon reaction of 2-(10β-dihydroartemisinoxy)ethylbromide with different aminoquinoline moieties under specific conditions and were shown to have moderate in vitro antimalarial activity.

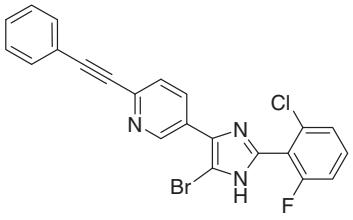

Assays	IC_{50} (nM)
mPGES-1	1
A549 (2%/50% FBS)	13 / 160
HWBA	1600

Biarylimidazoles were prepared and evaluated as inhibitors of microsomal prostaglandin E_2 synthase-1.

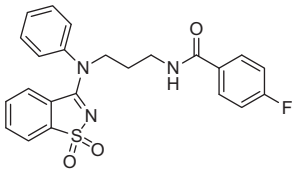

8b

We report the synthesis and in vitro activity of a series of novel *N*-{3-[(1,1-dioxido-1,2-benzothiazol-3-yl)(phenyl)amino]propyl}benzamide analogs. These analogs showed potent inhibitory activity against Kv1.3. Several compounds, including compound **8b**, showed similar potency to the known Kv1.3 inhibitor PAP-1 when tested under the IonWorks patch clamp assay conditions.

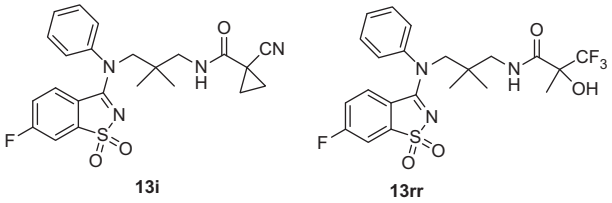

We report the synthesis and in vitro activity of a series of novel substituted *N*-{3-[(1,1-dioxido-1,2-benzothiazol-3-yl)(phenyl)amino] propyl}benzamide analogs. These analogs showed potent inhibitory activity against Kv1.3. Several demonstrated similar potency to the known Kv1.3 inhibitor PAP-1 when tested under the IonWorks patch clamp assay conditions. Two compounds, **13i** and **13rr**, were advanced further as potential tool compounds for in vivo validation studies.

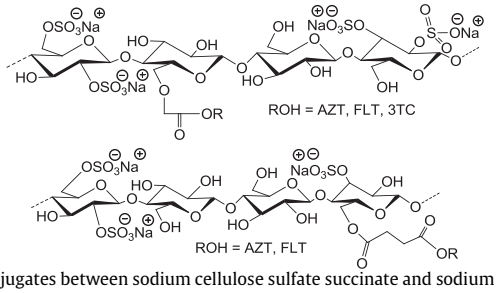

The synthesis and anti-HIV activities of two classes of conjugates between sodium cellulose sulfate succinate and sodium cellulose sulfate acetate as HIV-entry inhibitors and nucleoside reverse transcriptase inhibitors are reported.

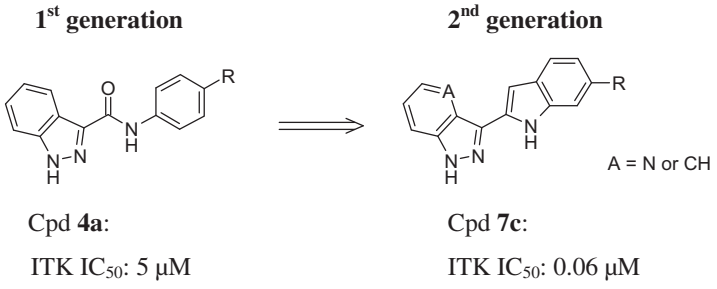

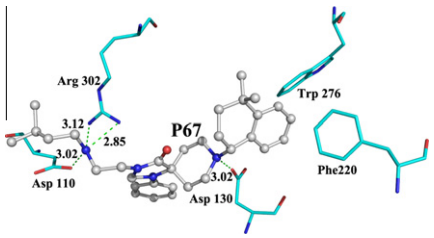

We studied 3D-QSAR and molecular mechanism of spiropiperidine analogues targeting nociceptin/orphanin FQ receptor (NOP). Molecular docking simulations reveal salt bridge, hydrogen-bonding, and hydrophobic interactions stabilize the most active agonist **P67** in the binding site pocket of NOP.

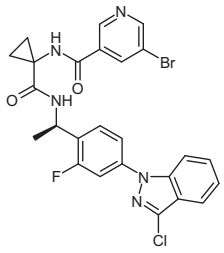

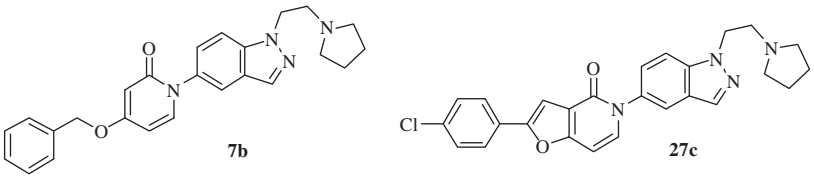

The synthesis and SAR of 5-(pyridinon-1-yl)indazoles and 5-(furopyridinon-5-yl)indazoles as potent MCH-1 antagonists are described.

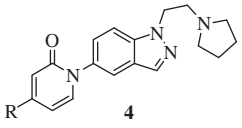

The synthesis and SAR of 4-aryl-1-(indazol-5-yl)pyridin-2(1*H*)ones as MCH-1 antagonists are described.

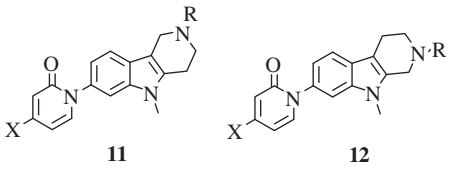

The synthesis and SAR of tetrahydrocarboline analogs as MCH-1 antagonists are described.

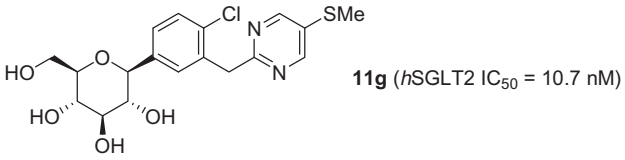

11g (*h*SGLT2 IC_{50} = 10.7 nM)

Novel *C*-aryl glucoside SGLT2 inhibitors containing pyrimidine motif were designed and synthesized for biological evaluation. Among various analogs tested, methylthiopyrimidine **11g** demonstrated best in vitro activity against *h*SGLT2 in this series to date.

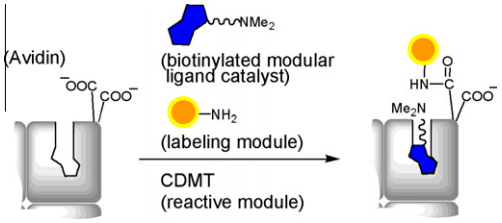

Mycoepoxydiene (MED) is a polyketide isolated from a marine fungus associated with mangrove forests. MED induced the reorganization of cytoskeleton in HeLa cells by promoting formation of actin stress fiber and inhibiting polymerization of tubulin. MED could induce cell cycle arrest at G2/M in HeLa cells. MED-associated apoptosis was characterized by the formation of fragmented nuclei, PARP cleavage, cytochrome *c* release, activation of caspase-3, and an increased proportion of sub-G1 cells. Additionally, MED activated MAPK pathways. It showed encouraging biological activities.

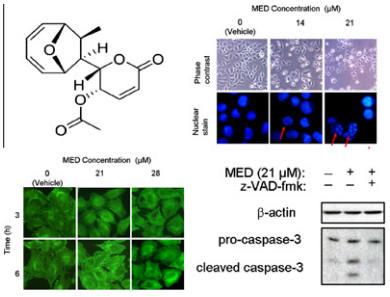

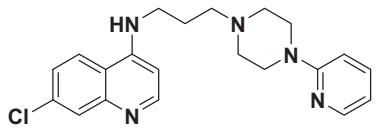

17, MIC = 0.125 μg/mL
Orally active at the dose 100 mg/kgx 4 days

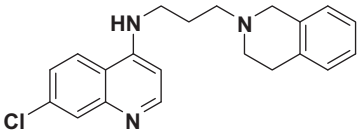

21, MIC = 0.031 μg/mL

New side chain modified 4-aminoquinolines and quinoline–acridine hybrids were synthesized and screened in vitro against NF 54 strain of *Plasmodium falciparum*. Compound **17** showed the curative response to all the treated mice infected with CQ-resistant N-67 strain of *Plasmodium yoelii* at the dose of 100 mg/kg for four days by oral route.

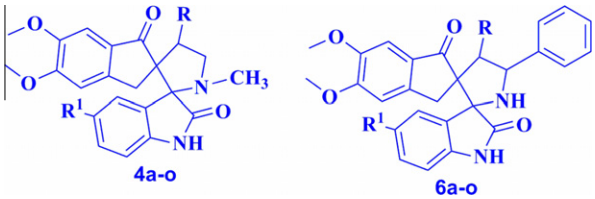

Compound **4k**, showed potent inhibitory activity against acetyl cholinesterase enzyme with IC_{50} 0.10 μmol/L. Pyrolidine analogues might be potential acetyl cholinesterase agents for AD.

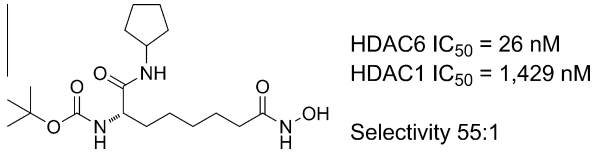

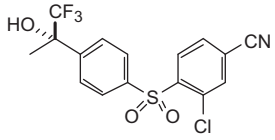

The synthesis and SAR of a series of diarylsulfone inhibitors of 11β-HSD1 are described. Optimization rapidly led to potent, selective, and orally bioavailable inhibitors demonstrating efficacy in a non-human primate ex vivo enzyme inhibition model.

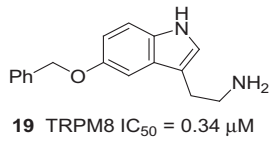

5-Benzyloxytryptamine **19** was found to be an antagonist of TRPM8. Related tryptamine derivatives showed diminished, or no activity at TRPM8.

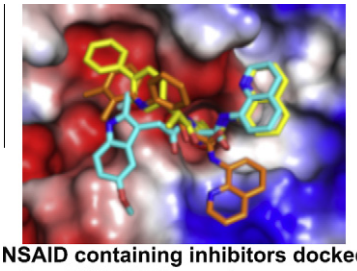

NSAID containing inhibitors docked into PfHDAC1 homology model.

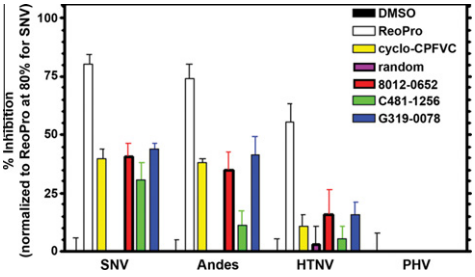

New entry inhibitors of hantaviruses that selectively target β_3 integrin, utilized by Andes and Sin Nombre virus, were selected using LBVS and cell-based assays. These bioactive compounds are thought to bind the receptor at host cell plasma membrane, thus preventing viral entry at the cell surface.

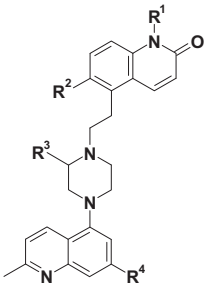

5-{2-[4-(2-Methyl-5-quinolinyl)-1-piperazinyl]ethyl}-2(1*H*)-quinolinones and 3,4-dihydro-2(1*H*)-quinolinones have been identified with different combinations of 5-HT$_1$ autoreceptor antagonist and hSerT potencies and excellent rat PK profiles. The availability of tool compounds with a range of profiles at targets known to play a key role in the control of synaptic 5-HT levels will allow exploration of different pharmacological profiles in a range of animal behavioral and disease models.

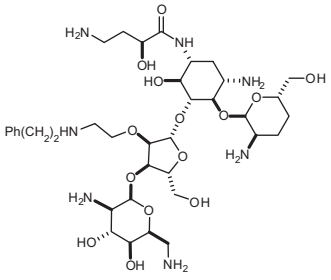

Incorporation of an hydrophobic (phenethylamino)ethyl ether at C2″ of N1-(HABA)-3′,4′-dideoxyparomomycin led to a novel analog with an excellent antibacterial profile against a host of resistant bacteria.

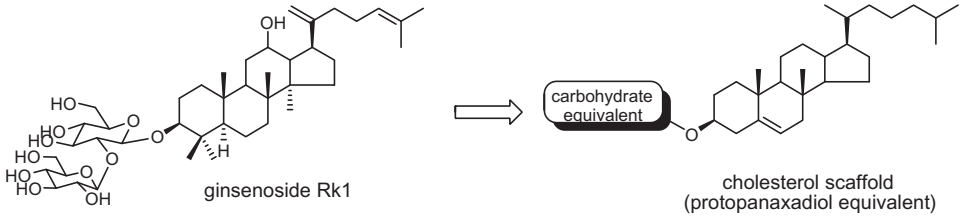

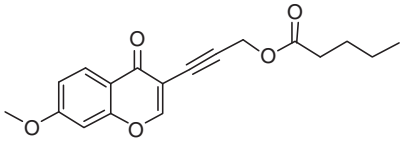

Compound 5j

A series of benzopyrones, NOE-azole antifungal agent, was synthesized and evaluated the antifungal activity in vitro, most of which showed moderate activity. Compound **5j** (MIC_{80} 1.5 μg/mL against *Trichophyton rubrum*) was the most potent one.

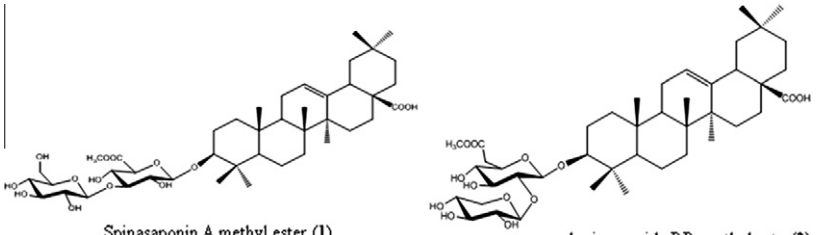

One newly (**1**) and 10 known oleanane-type triterpenoids were isolated from the methanol extract of *Panax stipuleanatus* rhizomes. Compounds **1** and **2** exhibited significant cytotoxic activity against two human cancer HL-60 and HCT-116 cell lines.

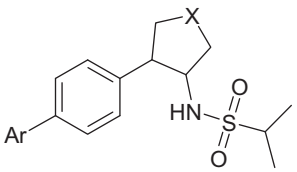

Ar = substituted phenyl or heterocycle.

This work describes the synthesis and biological activity of a series of pyrrolidine and tetrahydrofuran analogues as AMPA receptor positive modulators. Ar = substituted phenyl or heterocycle.

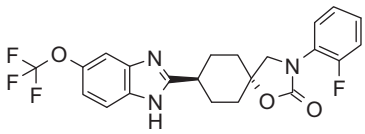

9b

The synthesis and SAR of a series of potent NPY Y5 antagonists is reported. Optimisation led to the identification of compounds **9b** (fpK_i = 9.2).

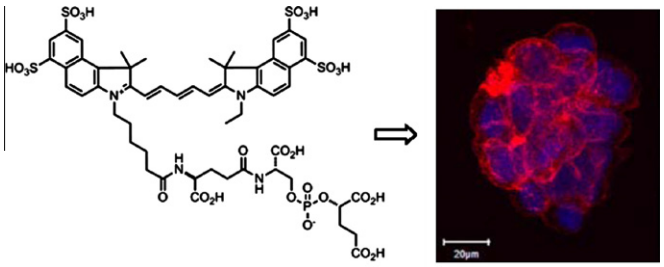

Cy5.5-CTT-54.2 **Tumor cell imaging**

A novel near-infrared imaging probe was synthesized, which exhibited potent PSMA inhibitory activity (IC_{50} = 0.55 nM) and PSMA-targeted imaging of prostate cancer cells in vitro.

A small library of novel benzocoumarin derivatives based on naturally occurring neo-tanshinlactone scaffold was constructed and some of them showed better activity then the reference compound tamoxifen.

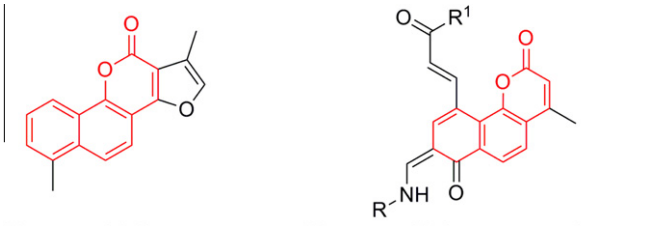

Neo-tanshinlactone (Naturally occurring)

Neo-tanshinlactone analogues (Synthetic)

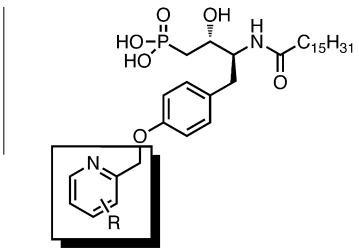

electron rich pyridyl region increases potency

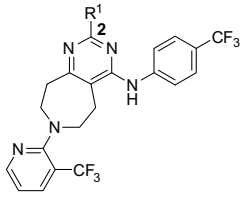

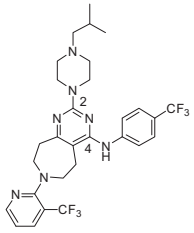

13
hTRPV1 IC_{50} = 11 ± 6 nM
rTRPV1 IC_{50} = 89 ± 43 nM

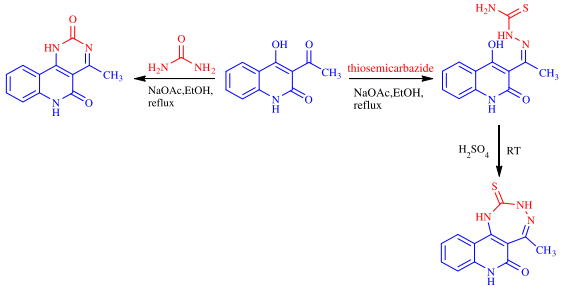

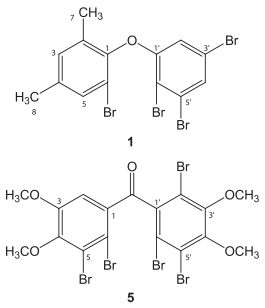

1

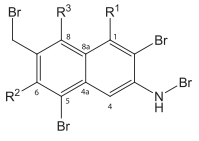

2 R^1=Br, R^2=H, R^3=H
3 R^1=H, R^2=H, R^3=Br
4 R^1=H, R^2=Br, R^3=H

5

*Corresponding author
Supplementary data available via ScienceDirect

COVER

Overlay of high resolution co-crystal structures of *R*-**22**-ADP (cyan) and **1**-ADP (green) bound in an allosteric binding site of the mitotic kinesin KSP. [Roecker, A. J.; Coleman, P. J.; Mercer, S. P.; Schreier, J. D.; Buser, C. A.; Walsh, E. S.; Hamilton, K.; Lobell, R. B.; Tao, W.; Diehl, R. E.; South, V. J.; Davide, J. P.; Kohl, N. E.; Yan, Y.; Kuo, L. C.; Li, C.; Fernandez-Metzler, C.; Mahan, E. A.; Prueksaritanont, T.; Hartman, G. D. *Bioorg. Med. Chem. Lett.* **2007**, *17*, 5677.]

Indexed/Abstracted in: Beilstein, Biochemistry & Biophysics Citation Index, CANCERLIT, Chemical Abstracts, Chemistry Citation Index, Current Awareness in Biological Sciences/BIOBASE, Current Contents: Life Sciences, EMBASE/Excerpta Medica, MEDLINE, PASCAL, Research Alert, Science Citation Index, SciSearch, TOXFILE. Also covered in the abstract and citation database SCOPUS®. Full text available on ScienceDirect®

ELSEVIER

ISSN 0960-894X